

Lattice damage produced in GaN by swift heavy ions

S. O. Kucheyev, H. Timmers, J. Zou, J. S. Williams, C. Jagadish, and G. Li

Citation: *Journal of Applied Physics* **95**, 5360 (2004); doi: 10.1063/1.1703826

View online: <http://dx.doi.org/10.1063/1.1703826>

View Table of Contents: <http://scitation.aip.org/content/aip/journal/jap/95/10?ver=pdfcov>

Published by the [AIP Publishing](#)

Articles you may be interested in

[Lattice damage and compositional changes in Xe ion irradiated \$\text{In}_x\text{Ga}_{1-x}\text{N}\$ \(\$x = 0.32-1.0\$ \) single crystals](#)
J. Appl. Phys. **119**, 245704 (2016); 10.1063/1.4954691

[Implantation-produced structural damage in \$\text{In}_x\text{Ga}_{1-x}\text{N}\$](#)
Appl. Phys. Lett. **79**, 602 (2001); 10.1063/1.1388881

[Fe ion implantation in GaN: Damage, annealing, and lattice site location](#)
J. Appl. Phys. **90**, 81 (2001); 10.1063/1.1377606

[Polycrystallization and surface erosion of amorphous GaN during elevated temperature ion bombardment](#)
J. Appl. Phys. **88**, 5493 (2000); 10.1063/1.1318361

[Strong surface disorder and loss of N produced by ion bombardment of GaN](#)
Appl. Phys. Lett. **76**, 3899 (2000); 10.1063/1.126814

The image shows the cover of an Applied Physics Reviews journal issue. It features a 3D schematic of a layered structure with labels for 'Substrate', 'Buffer layer', 'Active layer', and 'Gate dielectric'. Below the schematic is a graph showing a property versus a parameter. The cover also includes the AIP logo and the text 'Applied Physics Reviews' and 'apr.aip.org'.

NEW Special Topic Sections

NOW ONLINE
Lithium Niobate Properties and Applications:
Reviews of Emerging Trends

AIP Applied Physics
Reviews

Lattice damage produced in GaN by swift heavy ions

S. O. Kucheyev^{a)}

Lawrence Livermore National Laboratory, Livermore, California 94550

H. Timmers

School of Physics, University of New South Wales, Australian Defence Force Academy, Canberra, ACT 2600, Australia

J. Zou

Division of Materials and Centre for Microscopy and Microanalysis, The University of Queensland, Brisbane, QLD 4072, Australia

J. S. Williams and C. Jagadish

Department of Electronic Materials Engineering, Research School of Physical Sciences and Engineering, The Australian National University, Canberra, ACT 0200, Australia

G. Li

Ledex Corporation, No. 9, Ta-Yio First St., Ta-Fa Industrial District, Kaohsiung County, Taiwan, China

(Received 5 January 2004; accepted 18 February 2004)

Wurtzite GaN epilayers bombarded at 300 K with 200 MeV $^{197}\text{Au}^{16+}$ ions are studied by a combination of transmission electron microscopy (TEM) and Rutherford backscattering/channeling spectrometry (RBS/C). Results reveal the formation of near-continuous tracks propagating throughout the entire $\sim 1.5\text{-}\mu\text{m}$ -thick GaN film. These tracks, $\sim 100\text{ \AA}$ in diameter, exhibit a large degree of structural disordering but do not appear to be amorphous. Throughout the bombarded epilayer, high-resolution TEM reveals planar defects which are parallel to the basal plane of the GaN film. The gross level of lattice disorder, as measured by RBS/C, gradually increases with increasing ion fluence up to $\sim 10^{13}\text{ cm}^{-2}$. For larger fluences, delamination of the nitride film from the sapphire substrate occurs. Based on these results, physical mechanisms of the formation of lattice disorder in GaN in such a high electronic stopping power regime are discussed. © 2004 American Institute of Physics. [DOI: 10.1063/1.1703826]

I. INTRODUCTION

Recent extensive research of ion-beam processes in GaN has mainly focused on understanding production and properties of defects in this material under ion bombardment at keV energies. A number of unexpected and rather complex phenomena have been observed and studied, including a complex damage buildup and amorphization behavior, the formation of extended defects even at low temperatures (such as 77 K), preferential surface disordering, material decomposition, porosity, and efficient erosion. These processes have recently been reviewed in Refs. 1–3.

In all the previous studies,^{1–3} it has been assumed that lattice defects are produced as a result of nuclear (or elastic) collisions, while electronic energy loss processes (i.e., the excitation of the electronic subsystem of the solid) have a negligible role in defect formation in GaN under bombardment with keV ions.⁴ Indeed, in the case of irradiation with keV ions, the level of electronic excitation is $\leq 1\text{ keV/nm}$. Such low electronic energy losses typically do not result in the formation of lattice defects in radiolysis-resistant materials such as GaN.⁵

The level of electronic excitation gradually increases with increasing ion energy and atomic number. Electronic energy losses can reach some tens of keV/nm in the case of

heavy ions with energies of several hundred MeV. For example, with increasing energy of ^{197}Au ions from 300 keV up to 200 MeV, electronic energy loss in GaN increases from 1 up to 34 keV/nm, according to stopping powers from the TRIM code (version SRIM-2003.17).⁶ In this so-called *swift heavy ion* (SHI) bombardment regime, intense ultrafast excitation of valence electrons occurs along ion paths.

There have been numerous previous studies of SHI-induced damage in different solids. It has been found that SHI bombardment of various polymers and insulators results in the formation of *latent tracks*. Such tracks are continuous or discontinuous cylindrical damaged zones created along the paths of rapidly moving ions. Numerous experiments have shown that track formation processes are nonlinear. Indeed, tracks are created only when the level of electronic excitation exceeds a certain threshold, typically corresponding to electronic energy losses of $\sim 1\text{--}30\text{ keV/nm}$. Excellent reviews on the formation of latent tracks in polymers and insulators can be found in Refs. 7–9.

More recently, swift-ion-induced lattice damage has also been studied in metals (see, for example, Refs. 9 and 10) and a wide range of radiolysis-resistant semiconductors such as Si, Ge, GaAs, InP, InSb, GaSb, InAs, GeS, GaP, SiGe, SiC, UO_2 , Si_3N_4 , as well as AlN.^{11–16} After SHI irradiation, ion tracks have been observed by transmission electron microscopy (TEM) in some semiconductors including InSb, GaSb,

^{a)}Electronic mail: kucheyev1@llnl.gov

InP, GeS, SiGe, and Si_3N_4 .^{11–15} However, no tracks have been found in other materials such as Si, Ge, C (diamond), GaAs, GaP, AlN, and SiC.^{9,12,16} Ion tracks in some semiconductors (such as GeS, InP, Si_3N_4 , and GaSb)^{12,14,15} have been found to have an amorphous core, as in the case of many insulators.^{7–9} In other semiconductors (such as InSb, UO_2 , and SiGe),^{11–14} track cores consist of a disordered but not amorphous material.

In addition, the formation of amorphous tracks has recently been observed in Si,¹⁷ Ge,¹⁸ GaAs,¹⁹ and Al_2O_3 (Ref. 20) bombarded with 20–40 MeV C_{60} cluster (fullerene) ions. Note that, as discussed above, bombardment of Si, Ge, and GaAs with SHI does not result in track formation. This may be reconciled since a comparison of damage production in MeV fullerene and SHI irradiation regimes requires consideration of not only the total electronic stopping power but also the great difference in the velocities of SHI's and C_{60} ion clusters for the same energy loss. A detailed discussion of this so-called *velocity effect* has been given by Dammak *et al.*¹⁰ and will not be reproduced here.

In experiments on SHI-induced material modification, the key parameters of practical interest are (i) the threshold values of the stopping power required for track formation, (ii) track diameters, and (iii) defect structures inside the track. Several models have been developed to explain the transfer of the energy of electronic excitation into atomic motion, resulting in track formation in crystalline solids.²¹ The main models are the thermal spike,^{9,14,22} Coulomb explosion,^{7,23} and material instability at high levels of electronic excitation (i.e., lattice relaxation model).^{24,25} We will discuss the underlining physical processes of these three models in Sec. IV. Here, it should be noted that none of these models can *predict* the track formation behavior in semiconductors. It is likely that, in different solids, different physical mechanisms are responsible for track formation.

All the current models for track formation in semiconductors are nonpredictive. In particular, none of the current models describes the structural characteristics of the track core (i.e., the phase and defect structures in the lattice). It has often been assumed that the track core is completely amorphous, especially in wide band gap semiconductors.^{9,14} However, results of the present study as well as several previous reports^{11–14} show that it is not the case for many semiconductors. Hence, experiments are needed to reveal the response of each material to intense electronic excitation along SHI tracks.

While the physical processes following SHI bombardment of semiconductors are generally unclear, even less is known about the behavior of nitride semiconductors exposed to intense electronic excitation. Cylindrical amorphous tracks have previously been observed in Si_3N_4 bombarded with 710 MeV Bi ions.¹² In contrast, such irradiation has not resulted in track formation in AlN.¹² It is, therefore, interesting to consider whether intense electronic excitation can result in defect formation in GaN. Moreover, it may be possible to produce stoichiometric amorphous GaN by ion bombardment in the electronic stopping power regime and to study the properties of such an amorphous phase. Indeed, previous theoretical studies have predicted that amorphous GaN has

intriguing electronic properties.²⁶ As reported previously,^{27,28} GaN amorphized by keV ion bombardment, in the nuclear stopping power regime, exhibits material decomposition with the formation of nitrogen gas bubbles embedded into a Ga-rich matrix. This may not occur in the electronic stopping power regime of SHI's.

In this article, we present experimental data on the modification of GaN with SHI and discuss physical mechanisms of track formation in this material.

II. EXPERIMENT

The $\sim 1.5\text{-}\mu\text{m}$ -thick wurtzite undoped GaN epilayer used in this study was grown on a *c*-plane sapphire substrate by metal-organic chemical vapor deposition in a rotating disk reactor at Ledex Corporation, Taiwan. Samples, all cut from the same wafer, were bombarded with 200 MeV $^{197}\text{Au}^{16+}$ ions at 300 K with a beam flux of $\sim 3 \times 10^9 \text{ cm}^{-2} \text{ s}^{-1}$. Samples were exposed to fluences in the range from $\sim 6 \times 10^{10}$ up to $5 \times 10^{13} \text{ cm}^{-2}$. The Au beam was delivered by the NEC 14 UD pelletron accelerator at the Australian National University (ANU). In order to reduce sample heating during ion bombardment, the samples were mounted on a Cu holder with a conductive silver paste. The surface normal of the samples was at an angle of $\sim 4^\circ$ relative to the incident beam axis. The electronic and nuclear stopping powers of 200 MeV ^{197}Au ions in GaN are 34 and 0.31 keV/nm, respectively.⁶ The projected ion range is $\sim 12 \mu\text{m}$. Hence, these ions lose their energy predominantly in the electronic stopping power regime throughout the entire $\sim 1.5\text{-}\mu\text{m}$ -thick GaN film, while the ion end-of-range region is deep inside the sapphire substrate.

After implantation, samples were characterized *ex situ* at 300 K by Rutherford backscattering/channeling spectrometry (RBS/C) using an ANU 1.7 MV tandem accelerator (NEC, SSDH) with 3.3 MeV $^4\text{He}^+$ ions incident along the [0001] direction and backscattered into a detector at 168° relative to the incident beam direction. To characterize the microstructure of ion-beam-produced lattice defects, selected samples were studied by cross-sectional transmission electron microscopy (XTEM) in a Philips CM12 transmission electron microscope operating at 120 kV. Specimens for XTEM were prepared by 3.5 keV Ar^+ ion-beam thinning using a Gatan precision ion-polishing system. The high-resolution TEM (HRTEM) study was performed in a JEOL JEM-3000F electron microscope operating at 300 kV with a point resolution of 1.95 Å.

III. RESULTS

Figure 1 shows RBS/C spectra illustrating the damage buildup in GaN bombarded at 300 K with 200 MeV Au ions. It is seen from Fig. 1 that, with increasing ion fluence up to $\sim 10^{13} \text{ cm}^{-2}$, lattice disorder gradually accumulates roughly uniformly throughout the entire $\sim 1.5\text{-}\mu\text{m}$ -thick GaN film.²⁹ However, experiments show that bombardment to ion fluences above $\sim 10^{13} \text{ cm}^{-2}$ (for example, to fluences of 1.5, 2, and $\sim 5 \times 10^{13} \text{ cm}^{-2}$) results in the delamination of the GaN film from the sapphire substrate over the entire area irradiated ($\sim 4 \text{ mm}$ in diameter).

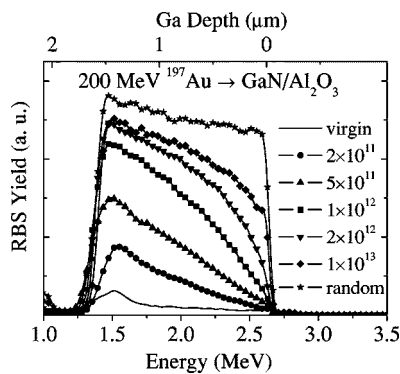


FIG. 1. Selected RBS/C spectra showing the damage buildup in GaN bombarded at 300 K with 200 MeV Au ions with a beam flux of $\sim 3 \times 10^9 \text{ cm}^{-2} \text{ s}^{-1}$. Ion fluences (in cm^{-2}) are indicated in the legend.

Figure 2 shows bright-field XTEM images of GaN bombarded at 300 K with 200 MeV Au ions to a fluence of $2 \times 10^{11} \text{ cm}^{-2}$. This figure illustrates the formation of near-continuous tracks, clearly visible even at low magnification. These tracks propagate throughout the entire GaN film into the sapphire substrate, which is consistent with previous studies of SHI-induced tracks in Al_2O_3 .¹² No external defects such as dislocations or stacking faults are visible in the vicinity of the tracks. Analysis of selected-area diffraction (SAD) patterns from the sample shown in Fig. 2 has not revealed the presence of an amorphous phase. Hence, the tracks appear to consist of a disordered material, resulting in lattice stress responsible for XTEM contrast.³⁰ The fluence of $2 \times 10^{11} \text{ cm}^{-2}$ corresponds to an average distance between ion impacts of $\sim 200 \text{ \AA}$. Hence, the areal density of tracks, revealed in Fig. 2, appears to be close to the density of ion impacts.

Tracks in Fig. 2 have an apparent diameter of $\sim 100 \text{ \AA}$. It should be noted, however, that, in the case when tracks are not amorphous, determination of track diameters from diffraction-contrast XTEM images can be ambiguous. Indeed, the size of the area exhibiting stress-induced XTEM contrast depends on imaging conditions. This can be seen from a comparison of Figs. 2(a) and 2(b), where the tracks

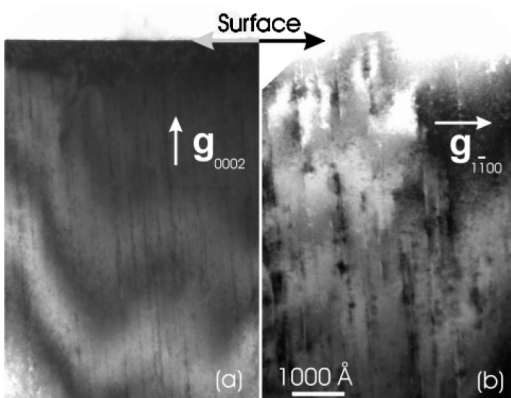


FIG. 2. Bright-field XTEM images [(a) $g=0002^*$ and (b) $g=1\bar{1}00^*$] of GaN bombarded at 300 K with 200 MeV Au ions with a beam flux of $\sim 3 \times 10^9 \text{ cm}^{-2} \text{ s}^{-1}$ to a fluence of $2 \times 10^{11} \text{ cm}^{-2}$. Both images are of the same magnification.

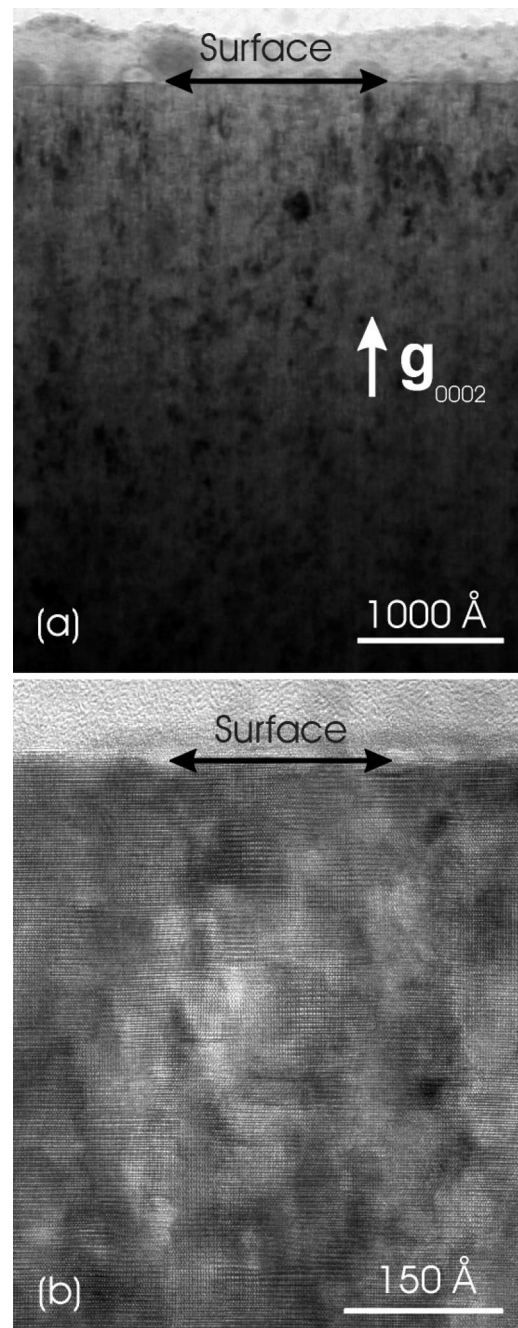


FIG. 3. (a) Bright-field XTEM image ($g=0002^*$) of GaN bombarded at 300 K with 200 MeV Au ions with a beam flux of $\sim 3 \times 10^9 \text{ cm}^{-2} \text{ s}^{-1}$ to a fluence of $1 \times 10^{13} \text{ cm}^{-2}$. (b) HRTEM image of the near-surface region of the sample depicted in (a).

appear slightly smaller in $g=0002^*$ images than in $g=1\bar{1}00^*$ taken from the same area of the cross-section. Hence, care should be exercised in the analysis of track diameters extracted from XTEM images in the case when tracks are not completely amorphous.

A bright-field XTEM image of a sample bombarded to a larger fluence of 10^{13} cm^{-2} is shown in Fig. 3(a). For this fluence, the average distance between ion impacts is $\sim 30 \text{ \AA}$. Hence, ion tracks effectively overlap, resulting in a rather uniform defect concentration throughout the entire GaN film. Our SAD analysis of this sample has revealed no evidence

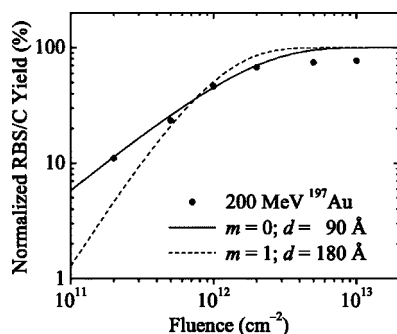


FIG. 4. Filled circles: ion fluence dependence of the RBS/C yield (at ~ 2.2 MeV), normalized to the random level, extracted from spectra such as those shown in Fig. 1. Curves: results of calculations based on the damage overlap model. The number of overlaps (m) and diameters of damage zones (d) are indicated in the legend.

for the presence of an amorphous phase. This result again supports the fact that the track core is damaged but not amorphous.

In order to better understand the structure of SHI-produced defects in GaN, samples have been studied by HRTEM. In agreement with results of the SAD studies discussed above, our HRTEM investigation has not revealed any amorphous phase in the GaN film. Figure 3(b) shows a HRTEM image illustrating the general view of structural defects in the same sample as shown in Fig. 3(a). Figure 3(b) reveals the presence of planar defects which are parallel to the basal plane of the GaN film. The average size of these planar defects is ~ 100 Å. Similar planar defects have previously been observed in GaN bombarded with keV ions.^{4,31,32}

IV. DISCUSSION

A. Damage accumulation

The mechanism of the damage buildup behavior can often be better understood by analyzing ion fluence dependencies of the level of lattice disorder, as measured by RBS/C. However, an accurate, nonspeculative extraction of the effective number of scattering centers from RBS/C spectra such as those shown in Fig. 1 is a rather challenging problem. Indeed, the atomic structure of the defects causing ion scattering is unknown. Moreover, the entire film has been damaged, which makes it difficult to quantitatively estimate the dechanneling component that arises from lattice strain surrounding defects. The damage buildup, however, can also be considered by plotting the RBS/C yield, normalized to the random level, as a function of ion fluence. Figure 4 (filled circles) shows such an ion fluence dependence of the normalized RBS/C yield at a depth of ~ 0.5 μm .

Damage buildup curves can often be described by the well-known defect overlap model developed in the 1970s.^{33–35} A detailed discussion of the defect overlap model can be found, for example, in Refs. 36 and 37. The model takes into account a spatial overlap of regions with an incompletely disordered crystal structure. It is assumed that an m -fold spatial overlap of incompletely disordered regions is required for complete lattice disordering. The basis of this model is the fact that the ratio of the surface area covered by

$(k-1)$ spatially overlapped disordered regions and the total area being irradiated can be described by the Poisson equation:

$$S_k = (a\Phi)^k \exp(-a\Phi)/k!, \quad (1)$$

where $a = \pi d^2/4$ is the area (projected on the surface of the crystal) of the disordered region at specific depth, Φ is ion fluence, and k is an integer number. In the case of $k=0$, S_0 determines the relative area of undamaged material. Based on Eq. (1), relative disorder in the crystal as a function of ion fluence can be written as

$$n_d = 1 - \exp(-a\Phi) \sum_{n=0}^m [(a\Phi)^n/n!]. \quad (2)$$

Results of fitting Eq. (2) to the data are shown in Fig. 4 by solid and dashed curves for 0 and 1 overlaps, respectively. It is seen from Fig. 4 that the best fit to experimental data is for parameters d and m of ~ 90 Å and 0, respectively. This corresponds to direct impact disordering (i.e., no spatial overlap of ion tracks is necessary to disorder the lattice, causing strong ion scattering and dechanneling). Note that the value of $d=90$ Å is in good agreement with the track diameters obtained from XTEM data from Fig. 2 (~ 100 Å).

Figure 4 also reveals that the normalized RBS/C yield (at ~ 2.2 MeV) exhibits a slow growth for ion fluences above $\sim 2 \times 10^{12}$ cm^{-2} , reaching a level of $\sim 80\%$ for a fluence of 10^{13} cm^{-2} . Such a slow increase in the RBS/C yield for relatively high ion fluences is not described by the simple defect overlap model (see Fig. 4). This reflects the complexity of the damage buildup in GaN under SHI bombardment and the oversimplification of the defect overlap model.³⁸ It should be noted that previous studies^{2,4,39,40} have revealed a rather complex damage buildup behavior in GaN under keV ion bombardment, including the effect of damage saturation in the crystal bulk. Figure 4 suggests that a somewhat similar damage saturation effect may also be present in GaN under SHI bombardment, but additional work is currently needed to clarify it.

B. Film delamination

It has previously been shown that irradiation with keV-GeV ions,⁴¹ 5–30 keV electrons,⁴² and 10–20 eV photons⁴³ often results in a significant enhancement of the adhesion of thin metal or semiconductor films on various substrates. Such an improvement in adhesion has been attributed to the energy deposition by irradiation into the electronic subsystem of the solid, leading to changes in local electron distribution and atomic configuration at film/substrate interfaces.^{41–43}

In contrast to the expected improvement of adhesion, the present study has revealed a catastrophic delamination of the GaN film from the sapphire substrate for ion fluences above $\sim 10^{13}$ cm^{-2} . Such a delamination can be attributed to ion-beam-induced rearrangement and weakening of atomic bonds at the film/substrate interface and the buildup of mechanical stress in both sapphire substrate and GaN film. Indeed, previous studies have shown that ion-beam-produced disorder results in material expansion and an associated

buildup of mechanical stress in GaN.^{27,28} It will be interesting to study damage produced in bulk GaN crystals by SHI irradiation to relatively large ion fluences ($\leq 10^{13}$ cm⁻²) when bulk GaN becomes readily available. Indeed, it is possible that due to its good mechanical properties,⁴⁴ bulk GaN will not exhibit disintegration for large fluences of SHI's.

C. Track formation mechanism

Since energy loss processes of energetic ions are relatively well understood and are similar for different crystals, the variations in the track formation behavior of different materials are mostly determined by processes of energy dissipation. As mentioned in Sec. I, the main *physical* models proposed to explain track formation in crystalline solids are the thermal spike,^{9,14,22} Coulomb explosion,^{7,23} and lattice relaxation^{24,25} models.

In the *thermal spike* model, excited electrons transfer their energy to atoms via the electron-phonon coupling. The amount of heat deposited into the thermal spike volume can be large, and the spike temperature can significantly exceed the melting point. Hence, a pseudoliquid ("molten") region is formed around the ion trajectory. Subsequent very rapid quenching of such a hot region results in the formation of an amorphous track if the cooling rate is too fast for epitaxial crystallization to occur. Imperfect recrystallization will result in the formation of a track consisting of a damaged but not amorphous material.

An alternative mechanism of track formation, related to thermal spikes, is *plastic deformation* due to the high pressure on the material surrounding the ion path. Indeed, heating of the track core material, after electrons transfer their energy to the lattice, results in thermal expansion and an associated stress field.

Within the *Coulomb explosion* model,^{7,23} a large density of positive charge in the track core results in repulsion between atoms, leading to atomic motion and track formation. Finally, according to the *lattice relaxation* model,^{24,25} intense electronic excitation weakens the covalent bonds and causes a repulsive force between atoms, resulting in collective atomic rearrangement and track formation.

Track formation in insulators has generally been explained within the Coulomb explosion approach,^{7,8,23} which has been supported by a number of experiments.⁴⁵ Tracks in semiconductors (which typically have chemical bonds with relatively low ionicities⁴⁶) have been attributed to the formation of thermal spikes.^{9,11-14,22,47} It should be noted, however, that there has been no direct experimental evidence to support the formation of thermal spikes along paths of SHI's in semiconductors. Miotello and Kelly⁴⁸ have recently given a detailed discussion of difficulties associated with using the thermal spike approach to describe the formation of latent tracks in solids under SHI bombardment. They have pointed out that, due to large kinetic energies of inner-shell electrons excited by a SHI,¹⁰ a large part of the energy deposited by the fast moving particle is carried away from the ion track volume and dissipated over larger distances, not confined by the ion trajectory. Hence, the existence of thermal spikes

along the trajectories of SHI's is not obvious, as also pointed out in another recent report.⁴⁹

Several attempts have previously been made to develop a theory which could predict the threshold ionization levels required for track formation in different materials.^{9,14} The authors of these models^{9,14} have tried to correlate the efficiency of track formation with fundamental parameters of the solid, such as the band gap, ionicity of chemical bonds, thermal conductivity, etc. However, similar to the case of lattice amorphization under keV ion bombardment,⁵⁰ none of the models proposed up to date can explain the influence of fundamental material parameters on track formation in different crystalline materials. Hence, it appears that a combination of material parameters can contribute to track formation efficiency, and more work is needed to better understand this process.

Based on our results as well as on results of the previous *ex situ* characterization studies of SHI-induced defects in crystals, it is difficult to answer the question of which physical mechanism is responsible for the formation of latent tracks in semiconductors. *In situ* experimental studies as well as a more sophisticated theoretical analysis would be desirable to shed light on the micromechanisms of track formation in GaN.

V. SUMMARY

In conclusion, we have studied the formation of structural defects in GaN bombarded at 300 K with 200 MeV Au ions. The main results of this work can be summarized as follows:

- (i) Near-continuous latent tracks, ~ 100 Å in diameter, have been observed.
- (ii) The core of these tracks consists of a damaged material, but it does not appear to be amorphous.
- (iii) Planar defects, ~ 100 Å in size, parallel to the basal plane of the GaN film have been observed.
- (iv) The damage buildup is best described by the direct impact (zero overlap) model.
- (v) For ion fluences above 10^{13} cm⁻², delamination of the GaN epilayer has been observed and attributed to ion-beam-induced rearrangement and weakening of atomic bonds at the film/substrate interface and the buildup of mechanical stress in both sapphire substrate and GaN film.

We have concluded that the *ex situ* experimental data currently available are not sufficient to conclusively decide on which physical processes are responsible for track formation in GaN and other semiconductors during SHI bombardment. Further work is thus needed to understand the micromechanisms responsible for track formation in GaN.

ACKNOWLEDGMENTS

The authors would like to thank A. Byrne for his contributions to ion bombardment experiments. This research was supported in part by the Australian Research Council. Work at LLNL was performed under the auspices of the U.S. Department of Energy by the University of California, Lawrence Livermore National Laboratory under Contract No. W-7405-Eng-48.

- ¹S. J. Pearton, J. C. Zolper, R. J. Shul, and F. Ren, *J. Appl. Phys.* **86**, 1 (1999).
- ²S. O. Kucheyev, J. S. Williams, and S. J. Pearton, *Mater. Sci. Eng., R.* **33**, 51 (2001).
- ³B. Rauschenbach, in *III-Nitride Semiconductors: Electrical, Structural and Defects Properties*, edited by M. O. Manasreh (Elsevier, Amsterdam, 2000), Chap. 7.
- ⁴S. O. Kucheyev, J. S. Williams, C. Jagadish, J. Zou, and G. Li, *Phys. Rev. B* **62**, 7510 (2000).
- ⁵See, for example, J. S. Williams, *Rep. Prog. Phys.* **49**, 491 (1986).
- ⁶J. F. Ziegler, J. P. Biersack, and U. Littmark, *The Stopping and Range of Ions in Solids* (Pergamon, New York, 1985).
- ⁷R. L. Fleischer, P. B. Price, and R. M. Walker, *Nuclear Tracks in Solids* (University of California Press, Berkeley, 1975).
- ⁸B. E. Fischer and R. Spohr, *Rev. Mod. Phys.* **55**, 907 (1983).
- ⁹F. F. Komarov, *Langmuir* **12**, 199 (1996).
- ¹⁰H. Dammak, A. Dunlop, D. Lesueur, A. Brunelle, S. Della-Negra, and Y. Le Beyec, *Phys. Rev. Lett.* **74**, 1135 (1995).
- ¹¹O. Herre, W. Welsch, E. Wendler, P. I. Gaiduk, F. F. Komarov, S. Klau-münzer, and P. Meier, *Phys. Rev. B* **58**, 4832 (1998).
- ¹²S. J. Zinkle, V. A. Skuratov, and D. T. Hoelzer, *Nucl. Instrum. Methods Phys. Res. B* **191**, 758 (2002).
- ¹³P. I. Gaiduk, A. N. Larsen, C. Trautmann, and M. Toulemonde, *Phys. Rev. B* **66**, 045 316 (2002).
- ¹⁴G. Szenes, Z. E. Horvath, B. Pecz, F. Paszti, and L. Toth, *Phys. Rev. B* **65**, 045 206 (2002).
- ¹⁵J. Vetter, *Radiat. Meas.* **25**, 33 (1995).
- ¹⁶S. A. Karamyan, *Nucl. Tracks Radiat. Meas.* **18**, 365 (1991).
- ¹⁷A. Dunlop, G. Jaskierowicz, and S. Della-Negra, *Nucl. Instrum. Methods Phys. Res. B* **146**, 302 (1998).
- ¹⁸A. Colder, O. Marty, B. Canut, M. Levalois, P. Marie, X. Portier, S. M. M. Ramos, and M. Toulemonde, *Nucl. Instrum. Methods Phys. Res. B* **174**, 491 (2001).
- ¹⁹A. Colder, B. Canut, M. Levalois, P. Marie, X. Portier, and S. M. M. Ramos, *J. Appl. Phys.* **91**, 5853 (2002).
- ²⁰S. M. M. Ramos, N. Bonardi, B. Canut, and S. Della-Negra, *Phys. Rev. B* **57**, 189 (1998).
- ²¹Note that the models discussed here are not limited to the case of crystalline solids but can also be applied to explain the track formation found in some amorphous materials such as metallic glasses, fused silica, and various polymers.
- ²²M. Toulemonde, C. Dufour, and E. Paumier, *Phys. Rev. B* **46**, 14 362 (1992).
- ²³R. L. Fleischer, P. B. Price, R. M. Walker, and E. L. Hubbard, *Phys. Rev.* **156**, 353 (1967).
- ²⁴P. Stampfli and K. H. Bennemann, *Phys. Rev. B* **42**, 7163 (1990).
- ²⁵P. Stampfli, *Nucl. Instrum. Methods Phys. Res. B* **107**, 138 (1996).
- ²⁶P. Stumm and D. A. Drabold, *Phys. Rev. Lett.* **79**, 677 (1997).
- ²⁷S. O. Kucheyev, J. S. Williams, C. Jagadish, V. S. J. Craig, and G. Li, *Appl. Phys. Lett.* **77**, 1455 (2000).
- ²⁸S. O. Kucheyev, J. S. Williams, J. Zou, C. Jagadish, and G. Li, *Appl. Phys. Lett.* **77**, 3577 (2000).
- ²⁹Note that the spectrum from a virgin (i.e., unirradiated) sample reveals an increased RBS/C yield near the GaN/Al₂O₃ interface. Such increased disorder is related to scattering from a thin GaN buffer layer grown at a low temperature as well as from an increased concentration of as-grown lattice defects near the epilayer/substrate interface.
- ³⁰It is also possible that, immediately after SHI bombardment, tracks are completely amorphous but experience recrystallization over the period up to several days after ion bombardment before the subsequent XTEM analysis. In addition, effective recrystallization of tracks could occur during electron beam irradiation in the TEM. It should also be noted that ion tracks in GaN are stable at room temperature. Indeed, an XTEM analysis of samples stored at 300 K over one year has revealed no changes in track size and density.
- ³¹C. M. Wang, W. Jiang, W. J. Weber, and L. E. Thomas, *J. Mater. Res.* **17**, 2945 (2002).
- ³²Y. G. Wang, J. Zou, S. O. Kucheyev, J. S. Williams, C. Jagadish, and G. Li, *Electrochem. Solid-State Lett.* **6**, G34 (2003).
- ³³J. F. Gibbons, *Proc. IEEE* **60**, 1062 (1972).
- ³⁴I. A. Abroyan, V. S. Belyakov, O. A. Podsvirov, and A. I. Titov, *Interaction of Atomic Particles with Solids. Proc. of All-Soviet Symposium* (MGU, Moscow, 1972), p. 296 (in Russian).
- ³⁵I. A. Abroyan, V. S. Belyakov, and A. I. Titov, *Mikroelektronika* **5**, 231 (1976) (in Russian).
- ³⁶W. J. Weber, *Nucl. Instrum. Methods Phys. Res. B* **166–167**, 98 (2000).
- ³⁷A. I. Titov, S. O. Kucheyev, V. S. Belyakov, and A. Yu. Azarov, *J. Appl. Phys.* **90**, 3867 (2001).
- ³⁸It should also be noted that the normalized RBS/C yield, plotted in Fig. 4, only approximately represents the damage buildup behavior.
- ³⁹W. Jiang, W. J. Weber, S. Thevuthasan, G. J. Exarhos, and B. J. Bozlee, *MRS Internet J. Nitride Semicond. Res.* **4S1**, G6.15 (1999).
- ⁴⁰W. Jiang, W. J. Weber, and S. Thevuthasan, *J. Appl. Phys.* **87**, 7671 (2000).
- ⁴¹See, for example, reviews by J. E. E. Baglin, *Nucl. Instrum. Methods Phys. Res. B* **65**, 119 (1992); P. A. Ingemarsson, *ibid.* **44**, 437 (1990).
- ⁴²I. V. Mitchell, J. S. Williams, P. Smith, and R. G. Elliman, *Appl. Phys. Lett.* **44**, 193 (1984).
- ⁴³I. V. Mitchell, G. Nyberg, and R. G. Elliman, *Appl. Phys. Lett.* **45**, 137 (1984).
- ⁴⁴S. O. Kucheyev, J. E. Bradby, J. S. Williams, C. Jagadish, M. Toth, M. R. Phillips, and M. V. Swain, *Appl. Phys. Lett.* **77**, 3373 (2000).
- ⁴⁵See, for example, G. Schiwietz, E. Luderer, G. Xiao, and P. L. Grande, *Nucl. Instrum. Methods Phys. Res. B* **175–177**, 1 (2001), and references therein.
- ⁴⁶J. C. Phillips, *Bonds and Bands in Semiconductors* (Academic, New York, 1973).
- ⁴⁷F. F. Komarov and V. A. Belyi, *J. Exp. Theor. Phys.* **95**, 316 (2002).
- ⁴⁸A. Miotello and R. Kelly, *Nucl. Instrum. Methods Phys. Res. B* **122**, 458 (1997).
- ⁴⁹E. Bringa and R. E. Johnson, *Phys. Rev. Lett.* **88**, 165501 (2002).
- ⁵⁰H. M. Naguib and R. Kelly, *Radiat. Eff.* **25**, 1 (1975).